Current density maps, magnetizability, and nuclear magnetic shielding tensors of bis-heteropentalenes. I. Di-hydro-pyrrolo–pyrrole isomers

I. García Cuesta
Departament de Química Física, Institut de Ciència Molecular, Universitat de València, 46100 Burjassot, València, Spain

R. Soriano Jartín
Dipartimento di Chimica dell'Università degli Studi di Modena e Reggio Emilia, 41100 Modena, Italy

A. Sánchez de Merás
Departament de Química Física, Institut de Ciència Molecular. Universitat de València, 46100 Burjassot, València, Spain

P. Lazzeretti
Dipartimento di Chimica dell'Università degli Studi di Modena e Reggio Emilia, 41100 Modena, Italy

(Received 29 May 2003; accepted 18 June 2003)

Magnetic susceptibility and nuclear magnetic shielding at the nuclei of bis-heteropentalenes formed by two pyrrole units ([2,3−*b*], [3,2−*b*], [3,4−*b*], and [3,4−*c*] isomers) have been evaluated by a series of different approximations and a large Gaussian basis set. An *ab initio* model of magnetic field induced current density was obtained for four isomeric systems, showing that strong diamagnetic flow takes place within the π electrons. The π currents are responsible for exalted magnetic anisotropy and proton deshielding. The theoretical findings are used to assess a diatropicity scale for these molecules. © *2003 American Institute of Physics.*
[DOI: 10.1063/1.1599337]

I. INTRODUCTION

Although aromaticity is customarily regarded on empirical grounds as ''something that everybody knows what it is,'' no simple definition of it is available. A number of more or less widely accepted benchmarks of aromaticity have been proposed. Some of them overlap,[1] others are orthogonal to one another,[2] all of them are, to some extent, arguable and uncertain.[3–5] Possibly aromaticity is a multi-dimensional phenomenon.[6,7]

Much attention has been paid to molecules containing two fused five-membered heterocyclic rings.[8–13] These systems were studied by Novak to establish their aromatic character by quantitative criteria.[14] Adopting Bird's[11,15,16] unified index $I_{5,5}$, the aromaticity of bis-heteropentalenes increases according to the sequence[14]

$$[3,4-b]\rightarrow[2,3-b]\rightarrow[3,2-b]\rightarrow[3,4-c]. \quad (1)$$

Subramanian *et al.*[17] investigated the connections between stability and aromaticity, and examined various measures of aromaticity for the fused hetero-bicycles. Adopting magnetic criteria as the preferential indicators, these authors argued that the most strongly aromatic systems show the least stable forms,[17] in contrast with previous findings.[8,13,18] Moreover, the most stable positional isomers, e.g., [3,2−*b*], need not have the largest aromatic or resonance stabilization.[17] The reliability of the hardness concept, as well as geometrical parameters as aromaticity indices has also been questioned by the same authors.[17]

In fact, both qualitative and quantitative indicators are needed to specify the vague and debatable notion of aromaticity. Useful information is provided by ab initio models of induced current densities, which directly visualize the diatropicity of a molecule.[19–22] According to the Ring-current model (RCM) of Pauling,[23] Lonsdale,[24] and London,[25,26] a magnetic field perpendicular to the molecular plane of benzene induces intense circulation of π electrons. Although these currents are not directly observable, reliable pictures of the charge flow can be obtained via computer experiments.

Maps showing streamlines and modulus of the current density yield valuable tools for interpreting the large out-of-plane component of the magnetic susceptibility and the proton deshielding.[3–5,20,22,27–30] The out-of-plane susceptibility and the magnetic anisotropy provide quantitative descriptors of diatropicity, in connection with the degree of delocalization of electron currents estimated qualitatively via plots of current intensity and streamlines.

These aspects constitute the object of the present study, which is meant to search evidence for the diatropicity of fused nitrogen-containing hetero-bicycles (**1**)–(**4**) and its possible connection with aromaticity.

II. COMPUTATIONAL DETAILS

The Gaussian basis sets adopted in the present investigations are the noncontracted $(13s8p4d)$ for C and N atoms, and $(8s3p)$ for H. The (s/p) substrata are from van Duijneveldt,[31] and the exponents of the polarization functions were chosen to maximize paramagnetic susceptibilities in smaller molecules.[32]

Molecular geometries were optimized by the GAUSSIAN code,[33] using the 6-31G* basis set within the B3LYP approach. The results evidenced that all the molecules except [3,4−*b*] are planar. The N_2-H_4 bond in this molecule is

 © 2003 American Institute of Physics

Downloaded 16 Mar 2004 to 147.156.122.171. Redistribution subject to AIP license or copyright, see http://jcp.aip.org/jcp/copyright.jsp

TABLE I. Bond lengths (Å).[a]

[3,4−*b*] Cs symmetry				[3,2−*b*] C2*h* symmetry			
N1–C1	1.372	N1–H6	1.003	C1–N1	1.386	C1–H1	1.081
C1–C2	1.385	C1–H1	1.075	N1–C6	1.380	N1–H5	1.007
C2–C4	1.438	C4–H2	1.076	C6–C5	1.397	C3–H3	1.081
C4–C6	1.365	C6–H3	1.077	C5–C3	1.424		
C6–N2	1.389	N2–H4	1.001	C3–C1	1.383		
N2–C3	1.379	C5–H5	1.074				
C3–C5	1.378						
C5–N1	1.382						
C2–C3	1.430						
[2,3−*b*] C2*v* symmetry				[3,4−*c*] D2*h* symmetry			
C1–N1	1.400	C1–H1	1.080	N1–C1	1.372	N1–H5	1.010
N1–C6	1.369	N1–H5	1.007	C1–C5	1.401	C1–H1	1.079
C6–C5	1.393	C3–H3	1.082	C5–C6	1.465		
C5–C3	1.436						
C3–C1	1.375						

[a]Experimental bond lengths for 1,4-Di-*tert*-butyl-1,4-dihydropyrrolo[3,2−*b*]pyrrole:$C_3-C_5=1.409$, $C_1-C_3=1.359$, $C_5-C_6=1.374$, $C_6-N_1=1.384$, $C_1-N_1=1.376$ Å, from Ref. 35.

tilted off the plane. However, the deviation from planarity estimated via 6-31G* basis set was quite small, less than ≈2 degrees, the lowest frequency being inside the error of the method. See scheme below.

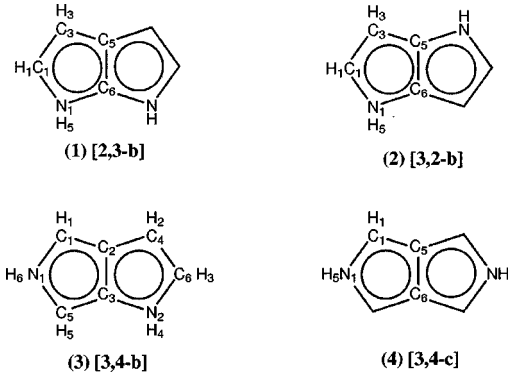

These findings are slightly at variance with those of Novak, who, employing a DZVP basis set,[34] and adopting the BLYP functional for geometry optimization, found that [2,3−*b*] and [3,2−*b*] systems are nonplanar, whereas [3,4−*b*] is predicted to be planar.[14] Small differences were found for the internal C–C bond lengths reported by Novak, 1.405, 1.411, 1.446, and 1.476 Å, respectively for **1**, **2**, **3**, and **4**. These estimates are slightly bigger than the corresponding values shown in Table I, 1.393, 1.397, 1.430, and 1.465 Å. However, bond lengths increase along the same **1**→**4** sequence. Experimental bond lengths from Ref. 35 for 1,4-Di-*tert*-butyl-1,4-di-hydro-pyrrolo[3,2−*b*]pyrrole have been reported in Table I.

The Pople basis sets[36] are known to give reasonable molecular geometries in DFT calculations. The DZVP basis sets[34] are of the same size as 6-31G*. Then the small differ-

TABLE II. Magnetic susceptibility tensor of nitrogen containing bis-heteropentalenes in (cgs) ppm a.u.[a] (origin in the center of mass). Anisotropy $\Delta\chi=\chi_{zz}-\frac{1}{2}(\chi_{xx}+\chi_{yy})$.

	xx	*yy*	*zz*	*xy*	*av*	$\Delta\chi$
[2,3−*b*]						
$\chi^{\Delta}+\chi^{p}$	−641.17	−576.58	−1427.54	0.00	−881.76	−818.67
$\chi^{d}+\chi^{\Pi}$	−645.15	−580.02	−1423.89	0.00	−883.02	−811.31
$\chi^{d}+\chi^{p}$ (LO)	−644.65	−580.77	−1426.30	0.00	−883.91	−813.59
[3,4−*b*]						
$\chi^{d}+\chi^{p}$ (LO)	−597.11	−600.35	−1423.40	0.07	−873.62	−824.67
[3,2−*b*]						
$\chi^{\Delta}+\chi^{p}$	−637.73	−573.72	−1460.03	16.96	−890.49	−854.30
$\chi^{d}+\chi^{\Pi}$	−641.38	−577.50	−1456.35	16.98	−891.74	−846.91
$\chi^{d}+\chi^{p}$ (LO)	−641.34	−578.20	−1459.00	16.58	−892.85	−849.23
[3,4−*c*]						
$\chi^{\Delta}+\chi^{p}$	−518.24	−605.73	−1624.89	0.00	−916.28	−1062.90
$\chi^{d}+\chi^{\Pi}$	−522.58	−608.56	−1619.86	0.00	−917.00	−1054.29
$\chi^{d}+\chi^{p}$ (LO)	−522.56	−609.08	−1623.69	0.00	−918.44	−1057.87

[a]The conversion factor from cgs a.u. per molecule to cgs emu per mole is $a_0^3 N_A=8.923\,8878\times10^{-2}$; further conversion to SI units is obtained by 1 $JT^{-2}=0.1$ cgs emu.

Downloaded 16 Mar 2004 to 147.156.122.171. Redistribution subject to AIP license or copyright, see http://jcp.aip.org/jcp/copyright.jsp

TABLE III. Nuclear magnetic shielding in 1,6-dihydro-pyrrolo[2,3−*b*]pyrrole (in ppm).

	xx	*yy*	*zz*	*xy*	*av*
N1					
σ (DZ2)	144.02	90.54	201.17	−12.85	145.24
σ (PZ2)	143.84	90.32	200.67	−12.85	144.95
σ (LO)	144.90	91.24	201.15	−12.78	145.77
C1					
σ (DZ2)	−5.20	71.42	137.83	33.88	68.02
σ (PZ2)	−5.63	71.24	137.40	33.76	67.67
σ (LO)	−4.96	72.02	137.92	34.03	68.33
C3					
σ (DZ2)	33.70	36.47	173.84	52.12	81.34
σ (PZ2)	33.41	36.34	173.58	52.23	81.11
σ (LO)	34.15	36.80	173.89	52.37	81.62
C5					
σ (DZ2)	18.06	43.58	160.80	0.00	74.15
σ (PZ2)	17.81	43.37	160.49	0.00	73.89
σ (LO)	18.52	44.05	160.73	0.00	74.43
C6					
σ (DZ2)	−30.77	43.12	123.78	0.00	45.38
σ (PZ2)	−31.13	42.39	123.25	0.00	44.84
σ (LO)	−30.16	43.88	123.69	0.00	45.80
H1					
σ (DZ2)	27.56	26.14	20.68	−0.42	24.80
σ (PZ2)	27.71	26.24	20.72	−0.47	24.89
σ (LO)	27.83	26.51	20.95	−0.43	25.10
H3					
σ (DZ2)	25.99	27.57	21.38	0.05	24.98
σ (PZ2)	26.07	27.72	21.29	0.06	25.03
σ (LO)	26.35	27.83	21.63	0.16	25.27
H5					
σ (DZ2)	25.12	31.34	16.15	3.00	24.20
σ (PZ2)	25.20	31.57	16.25	3.06	24.34
σ (LO)	25.70	31.73	16.52	2.90	24.65

TABLE IV. Nuclear magnetic shielding in 1,4-dihydro-pyrrolo[3,2−*b*]pyrrole (in ppm).

	xx	*yy*	*zz*	*xy*	*av*
N1					
σ (DZ2)	123.33	82.64	205.26	−29.79	137.08
σ (PZ2)	123.07	82.38	204.76	−29.81	136.74
σ (LO)	124.21	83.37	205.24	−29.85	137.61
C1					
σ (DZ2)	−13.02	55.84	140.10	37.82	60.97
σ (PZ2)	−13.53	55.63	139.66	37.76	60.59
σ (LO)	−12.81	56.40	140.21	38.03	61.27
C3					
σ (DZ2)	53.17	51.42	174.63	36.10	93.07
σ (PZ2)	52.98	51.33	174.36	36.18	92.89
σ (LO)	53.68	51.66	174.67	36.28	93.34
C5					
σ (DZ2)	−10.73	36.98	140.18	−12.81	55.48
σ (PZ2)	−11.05	36.49	139.78	−12.67	55.07
σ (LO)	−10.22	37.64	140.08	−12.91	55.83
H1					
σ (DZ2)	27.10	25.89	20.45	0.41	24.48
σ (PZ2)	27.24	25.99	20.51	0.40	24.58
σ (LO)	27.37	26.25	20.70	0.44	24.77
H3					
σ (DZ2)	26.36	28.04	21.19	−0.01	25.19
σ (PZ2)	26.45	28.18	21.25	−0.02	25.29
σ (LO)	26.72	28.29	21.49	0.01	25.50
H5					
σ (DZ2)	25.07	31.23	15.87	2.16	24.06
σ (PZ2)	25.15	31.48	15.98	2.23	24.20
σ (LO)	25.64	31.63	16.25	2.07	24.51

ences between our predictions and Novak's[14] may depend on the type of DFT functional, rather than on the flexibility of the basis set retained for geometry optimization. Owing to the superior overall performance of the B3LYP functional versus BLYP, we are confident that planar geometries for [2,3−*b*] and [3,2−*b*] are more likely.

To further investigate if the structure of the [3,4−*b*] molecule is actually nonplanar, a systematic search for optimal geometry was carried out via basis sets of increasing size. The largest basis employed is cc-pVTZ.[37] The molecular energy differences observed via different basis sets are very small, and the inversion frequency of the N_2-H_4 bond always lies within the error. In any event, the degree of planarity increases on increasing basis set quality, which can be related to improved description of the vibrational mode for inversion at N atom.

Eventually, retaining the cc-pVTZ basis set, the molecule is predicted exactly planar with C_s symmetry, in agreement with Ref. 14. A subsequent calculation to check the stability of the wave function confirmed planarity.

The optimized bond lengths are shown in Table I. They have been employed in the calculation of magnetic properties and maps via the SYSMO code.[38]

Several different approximations relying on gaugeless basis sets $(13s8p4d)$ and $(8s3p)$ were tested at the Hartree–Fock (HF) level, e.g., the common origin (CO) approach and four procedures adopting a method first proposed by Keith and Bader,[39–42] based on continuous transformation of the origin of the currents density (CTOCD), which formally annihilate either diamagnetic (DZ) or paramagnetic (PZ) contributions. DZ2 and PZ2 variants employ damping factors to improve the accuracy of computed magnetic shielding. A description of CTOCD methods can be found in Refs. 5, 43–45, and 48–51.

The approach based on London orbitals (LO),[25,46] also referred to as gauge-including atomic orbitals (GIAO),implemented in the DALTON package,[47] has also been used.

A. Magnetic susceptibilities

The CTOCD-DZ and CTOCD-PZ values for magnetic susceptibility of 1,4-di-hydro-pyrrolo[3,2−*b*]pyrrole and [3,4−*c*] isomer, having vanishing electric dipole moment, are invariant in a gauge translation, whereas those for 1,5-di-hydro-pyrrolo[3,4−*b*]pyrrole and 1,6-di-hydro-pyrrolo[2,3−*b*]pyrrole depend on the coordinate system to which they are referred.

In any event, the quality of the $(13s8p4d/8s3p)$ basis is high enough to guarantee virtual origin independence of computed magnetic susceptibility and charge conservation. The relationships for origin independence were checked.[5] The average Thomas–Reiche–Kuhn sum rule is 55.7 for systems (**1**), (**2**), and (**4**), e.g., ≈99% of the total number of electrons, 56.

Downloaded 16 Mar 2004 to 147.156.122.171. Redistribution subject to AIP license or copyright, see http://jcp.aip.org/jcp/copyright.jsp

TABLE V. Nuclear magnetic shielding in 1,5-dihydro-pyrrolo[3,4−*b*]pyrrole (in ppm) via GIAO basis set.

	xx	*yy*	*zz*	*xy*	*av*
N1	9.40	129.92	187.05	−13.81	108.79
N2	155.95	131.19	200.74	−13.38	162.62
C1	65.72	20.55	156.41	−5.42	80.89
C2	31.13	2.98	156.59	26.45	63.56
C3	11.73	2.27	138.38	−40.85	50.80
C4	43.19	52.72	173.30	43.20	89.74
C5	83.92	48.21	157.58	7.43	96.57
C6	−25.33	47.65	135.45	59.57	52.59
H1	26.54	28.40	20.34	−0.31	25.10
H2	26.62	28.34	21.92	0.15	25.63
H3	26.65	26.50	21.18	1.70	24.78
H4	26.85	33.23	16.96	2.29	25.68
H5	26.90	28.68	20.46	0.09	25.35
H6	31.44	24.70	16.34	−0.72	24.16

Theoretical predictions for magnetic susceptibility are shown in Table II. The CO results from the gaugeless $(13s8p4d/8s3p)$ are comparatively less accurate and are not displayed. LO–CO values are partitioned into diamagnetic, χ^d, and paramagnetic, χ^p, contributions evaluated with respect to the center of mass (c.m.).

The least symmetric molecule of the series, 1,5-di-hydro-pyrrolo[3,4−*b*]pyrrole, has been studied only via the LO approach of the DALTON program,[47] because of the limitations affecting the present release of SYSMO package for molecules with low point group symmetry.[38]

Theoretical magnetic susceptibilities are expressed in ppm cgs atomic units. Total $\chi_{\alpha\beta}$, reported with five significant figures, is the algebraic sum of much larger diamagnetic and paramagnetic contributions, which introduces cancellation of errors affecting accuracy in reduced basis set calculations. For that reason, we have attempted to achieve near HF quality by estimating total magnetizability via different computational schemes.

Comparison of LO, DZ, and PZ results shows that there is virtually no difference among them, the predictions being closer than 1% in all cases. Therefore, the present findings can be used for a reliable guess of relative diatropicity of N-containing bis-heteropentalenes.

It can be observed in Table II that the out-of-plane component χ_{zz} increases, in absolute value, in the same direction as the sequence (1).[14] However, virtually identical values are predicted for 1,6-di-hydro-pyrrolo[2,3−*b*]pyrrole and 1,5-dihydro-pyrrolo[3,4−*b*]pyrrole. On the other hand, the theoretical anisotropy $\Delta\chi=\chi_{zz}-(1/2)(\chi_{xx}+\chi_{yy})$ of [3,4−*b*] is bigger than that of [2,3−*b*]. Interestingly enough, the trend of anisotropies is the same as for the Bird $I_{5,5}$ index reported in Table 5 by Novak.[14]

The theoretical results document the enhanced diatropicity of the bicyclic molecules 1,6-dihydro-pyrrolo[2,3−*b*]-pyrrole, 1,5-dihydro-pyrrolo[3,4−*b*]pyrrole, 1,4-dihydro-pyrrolo[3,2−*b*]pyrrole, and [3,4−*c*] isomer, recalling that the experimental $\Delta\chi$ of benzene is 669.1±1 (cgs) ppm a.u.[52] In fact, the average in-plane components are, in absolute value, from two to three times smaller than the out-of-plane component, which suggests that these bis-heteropentalenes could be classified as aromatic molecules on the basis of magnetic criteria, in accordance with Ref. 17.

TABLE VI. Nuclear magnetic shielding in the [3,4−*c*] isomer (in ppm).

	xx	*yy*	*zz*	*xy*	*av*
N1					
σ (DZ2)	−77.86	70.37	186.49	0.00	59.67
σ (PZ2)	−78.81	69.92	185.90	0.00	59.00
σ (LO)	−77.31	71.01	186.55	0.00	60.09
C1					
σ (DZ2)	64.80	42.76	155.14	12.06	87.57
σ (PZ2)	64.54	42.61	154.75	12.25	87.30
σ (LO)	65.42	42.98	155.28	12.10	87.89
C5					
σ (DZ2)	30.61	−15.54	161.11	0.00	58.73
σ (PZ2)	30.45	−16.05	160.78	0.00	58.39
σ (LO)	31.32	−15.26	160.94	0.00	59.00
H1					
σ (DZ2)	25.77	28.07	19.19	0.19	24.35
σ (PZ2)	25.85	28.24	19.24	0.21	24.45
σ (LO)	26.16	28.36	19.48	0.22	24.67
H5					
σ (DZ2)	27.16	23.32	14.72	0.00	21.73
σ (PZ2)	27.41	23.39	14.82	0.00	21.87
σ (LO)	27.54	23.89	15.06	0.00	22.16

B. Nuclear magnetic shieldings

Theoretical nuclear magnetic shieldings from CTOCD and LO methods are shown in Tables III–VI. The results are independent of the origin of the coordinate system. DZ2, PZ2, and LO magnetic shieldings of H, C, and N nuclei in (**1**), (**2**), and (**4**) are very close to one another, or almost identical in most cases, which proves the near HF accuracy of the calculation. CO predictions converge more slowly to the limit and are not shown. The excellent performance of CTOCD methods documented by these investigations gives additional evidence of their practicality for large molecular systems. In particular, gaugeless DZ2 and PZ2 schemes are competitive with GIAOs.

Calculated proton magnetic shieldings are frequently used for qualitative evaluation of the aromatic/antiaromatic character of planar conjugated systems.[4,5] For instance, the out-of-plane component of the shielding tensor in planar C_6H_6 isomers is affected by ring currents to different extent, which gives an estimate of their relative diatropicity.[30,53] On the other hand, the paratropic character of *s*-indacene is readily attributed to π-ring currents that provide an extra shielding as large as ≈5 ppm to σ_{zz}^{H3}.[54]

As regards the bis-heteropentalenes investigated in this work, the most deshielded out-of-plane components are those for H nuclei directly bonded to N, that is, H_5 in (**1**), (**2**), and (**4**), and for H_4 and H_6 in (**3**). The largest paramagnetic shift with respect to the theoretical $\sigma_{zz}^{H}=20.65$ ppm in benzene, see Table 6 of Ref. 55, was predicted to occur for H_5 in (**4**). It amounts to ≈−5 ppm, and it is mainly due to local deshielding exerted by the neighbor N atom.

The deshielding effect of N atom on the out-of-plane shielding component of an H atom bonded to a nearby C can also be observed, see, for instance, the results for H_1 in (**1**), (**2**), and (**3**), which are all characterized by a σ_{zz}^{H} very close

Downloaded 16 Mar 2004 to 147.156.122.171. Redistribution subject to AIP license or copyright, see http://jcp.aip.org/jcp/copyright.jsp

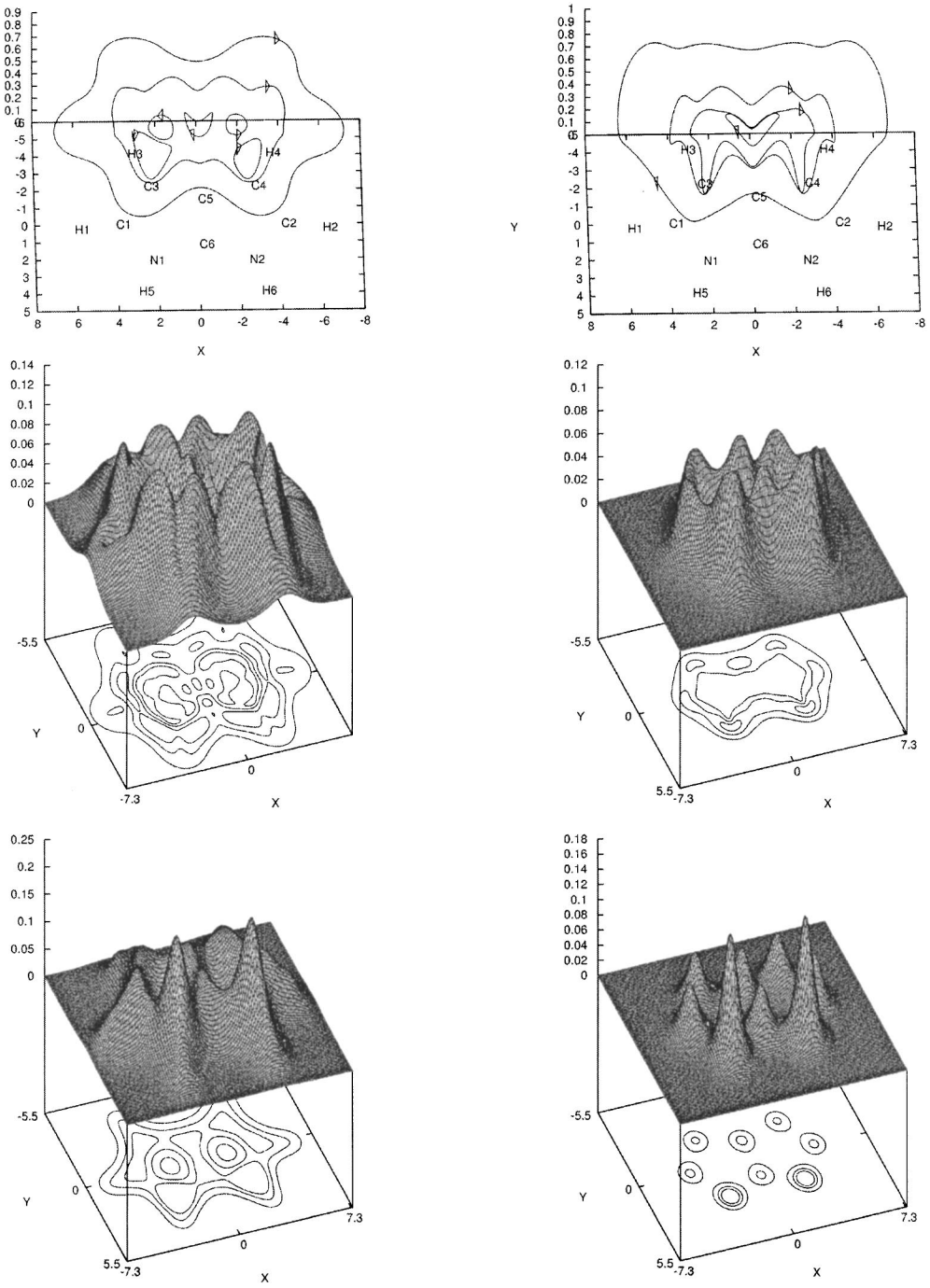

FIG. 1. The ring-current model for 1,6-dihydro-pyrrolo[2,3−*b*]pyrrole (**1**). From top to bottom, representations of the streamlines of the current density vector field **J** induced in the region of maximum π electron density by a magnetic field of unit magnitude along the positive *z* direction at right angles to the molecular plane, of its modulus, $|\mathbf{J}|$, and of ρ, the unperturbed electron charge density (in a.u.). Diamagnetic circulation is clockwise. The plots display a 3D-perspective view at points in planes parallel to the plane of the molecule, displaced from it by 0.8 bohr. Corresponding contour maps are shown with values $0.02n$, $n=0,1,2,...$ for $|\mathbf{J}|$, and $0.05n$, $n=0,1,2,...$ for the charge density. The maps on the left are relative to the total electronic distribution, those on the right are for the π-electron contribution.

to that of benzene. However, the H_1 proton in the [3,4−*c*] isomer is further deshielded, by ≈1.2 ppm, with respect to benzene's. The source of the additional paramagnetic shift is easily discovered with the help of Figs. 3 and 4, where a strong diamagnetic vortex is observed in the proximity of the adjacent N nucleus. It is this diamagnetic circulation that causes additional deshielding of σ_{zz}^{H1} in the [3,4−*c*] isomer.

The role played by the π-ring currents on magnetic shielding of H atoms bonded to C, and separated from the N nuclei by more than one bond, can be assessed by inspection of Tables III–VI. The σ_{zz}^{H} of H_3 in (**1**) and (**2**) is larger than that of benzene by ≈1 ppm. This would imply that the ring currents are slightly more intense in C_6H_6 than in 1,6-dihydro-pyrrolo[2,3−*b*]pyrrole and in 1,4-dihydro-pyrrolo[3,2−*b*]pyrrole.

No special effect can be attributed to ring currents in the

Downloaded 16 Mar 2004 to 147.156.122.171. Redistribution subject to AIP license or copyright, see http://jcp.aip.org/jcp/copyright.jsp

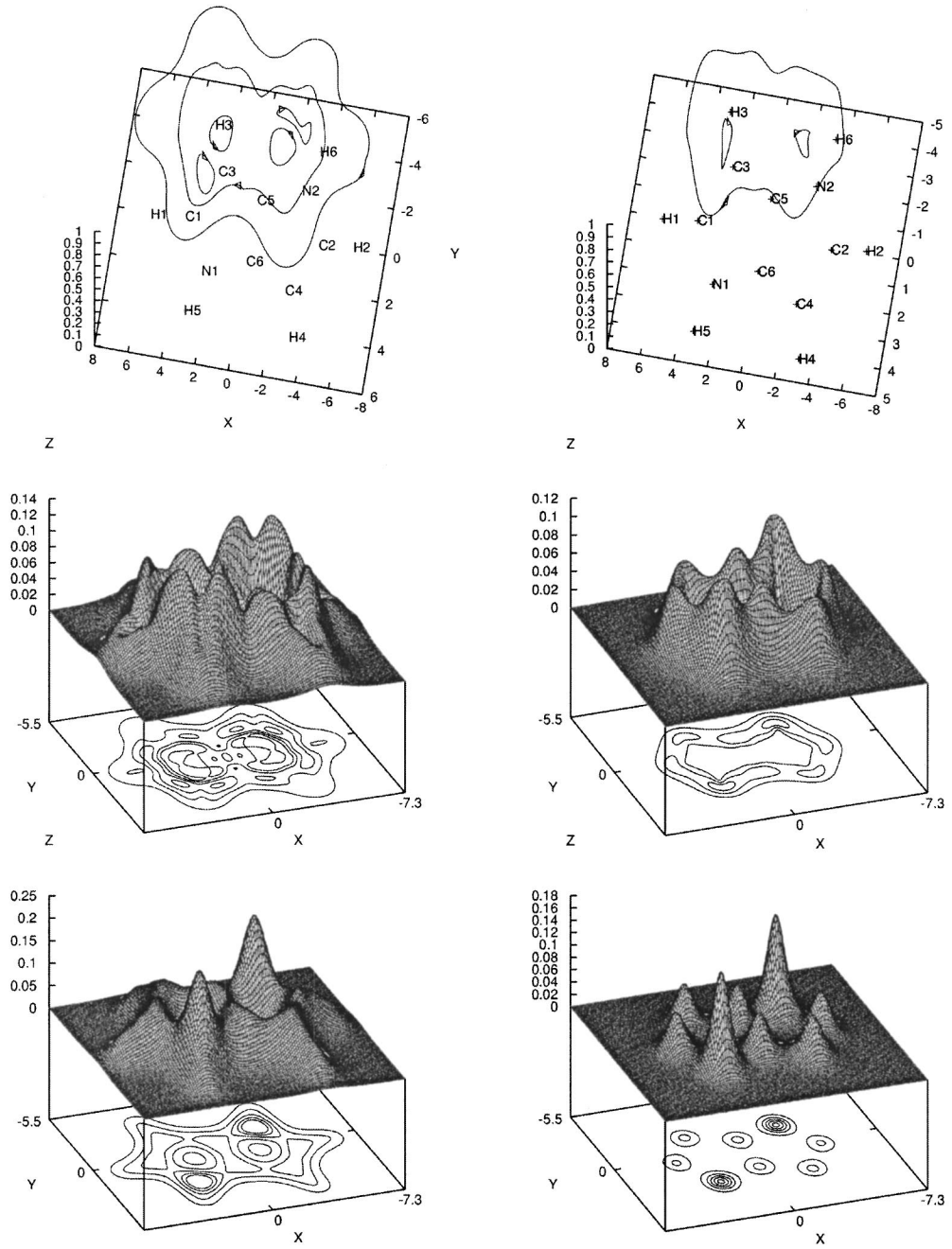

FIG. 2. The ring-current model for 1,4-dihydro-pyrrolo[3,2−*b*]pyrrole (**2**). The conventions are the same as in Fig. 1.

case of C and N nuclei lying along the molecular perimeter of bis-heteropentalenes. At any rate, the most shielded component is invariably the out-of-plane σ_{zz}. Another interesting finding, quite difficult to rationalize, is that the average in-plane component of N shielding in the [3,4−*c*] isomer almost vanishes.

C. Diatropicity and aromaticity of dihydro-pyrrolo–pyrroles

It might happen that the [3,4−*c*] isomer is least aromatic even if it shows the strongest diamagnetic ring currents. In fact, the computed self-consistent field (SCF) energies from the $(13s8p4d/8s3p)$ basis are −339.675 262, −339.679 212, −339.672 605, and −339.636 890 hartree, respectively, for (**1**), (**2**), (**3**), and (**4**). Then, at the SCF level of accuracy, the [3,4−*c*] isomer is less stable than the others. Correlation effects have also been taken into account at the B3LYP/cc-p VTZ level, confirming that the [3,4−*c*] isomer is the less stable one.

Both large diatropicity and small topological resonance energy (TRE) of this isomer can be derived consistently from Aihara graph theory.[56–61] Isomer [3,4−*c*] has the smallest TRE and the largest diatropic current along the periphery of the molecule. Thus, large diatropic ring currents are compatible with small aromatic stabilization energy. According to Refs. 57–61, ring currents can be partitioned among all pos-

Downloaded 16 Mar 2004 to 147.156.122.171. Redistribution subject to AIP license or copyright, see http://jcp.aip.org/jcp/copyright.jsp

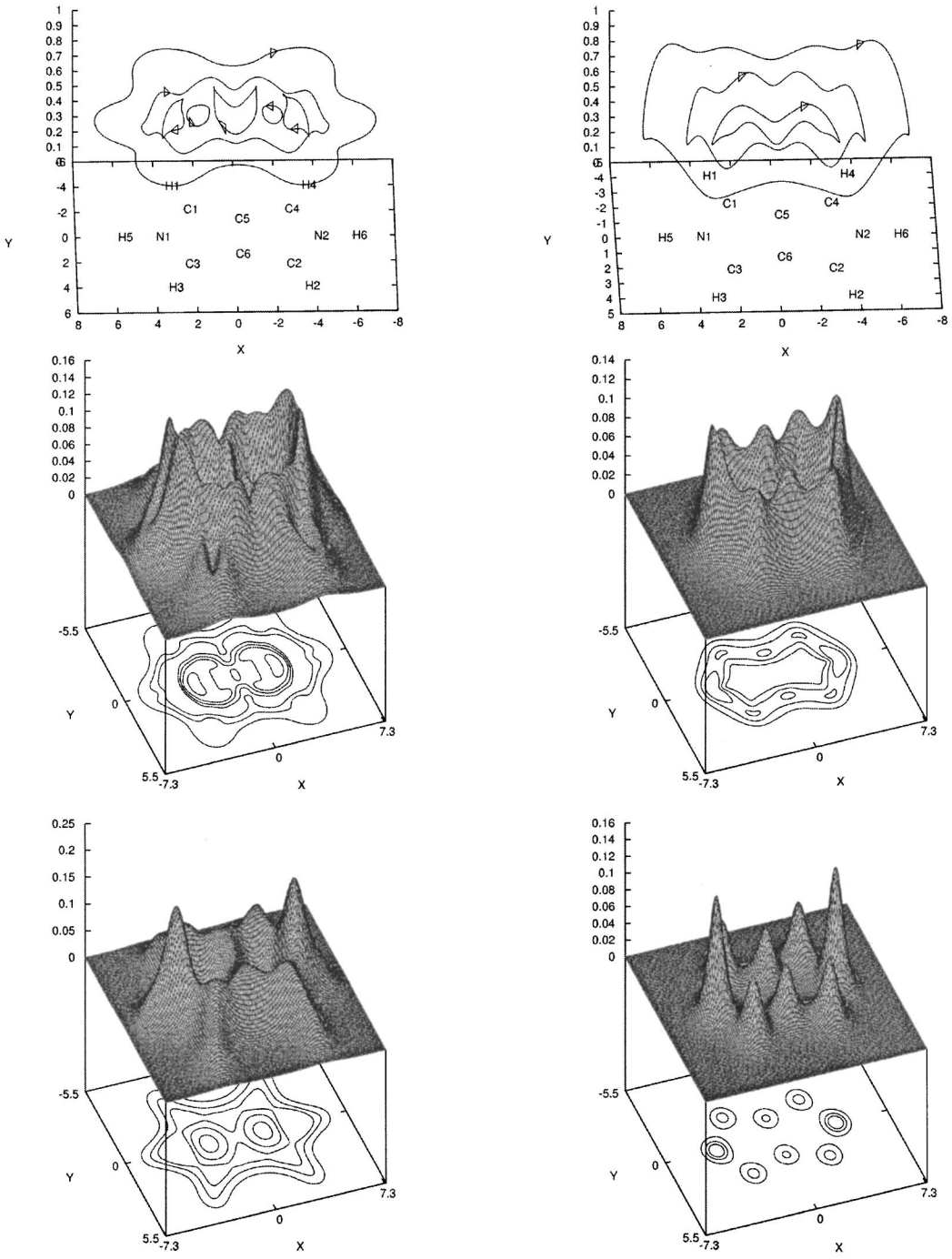

FIG. 3. The ring-current model for the $[3,4-c]$ isomer (**4**). The conventions are the same as in Fig. 1.

sible circuits. In other words, ring currents are given at the limit of zero magnetic field as a superposition of currents induced independently in the three circuits of dihydropyrrolo–pyrrole: two five-membered circuits and one eight-membered circuit. In the case of $[2,3-b]$ and $[3,2-b]$, strong diatropic currents are induced in the two five-membered circuits.

In marked contrast, in the case of $[3,4-c]$, the strongest diatropic current is induced in the eight-membered circuit. It should be noted, however, that larger circuits contribute less to aromaticity.[62] Therefore, it may in general be difficult to predict the degree of aromaticity from the ring current intensities or diamagnetic susceptibility exaltation. In this sense, the interpretation of NICS (Nucleus Independent Chemical Shift) values given in Ref. 17 is also questionable. Aihara's theory indicates explicitly that both aromatic stabilization and diatropicity can be interpreted consistently, but that these quantities are never proportional to each other.

In the light of these arguments, the sequence (1), for the increase in absolute value of the out-of-plane component of the magnetic susceptibility χ_{zz}, *does only account for relative diatropicities, not for aromaticities*.

Downloaded 16 Mar 2004 to 147.156.122.171. Redistribution subject to AIP license or copyright, see http://jcp.aip.org/jcp/copyright.jsp

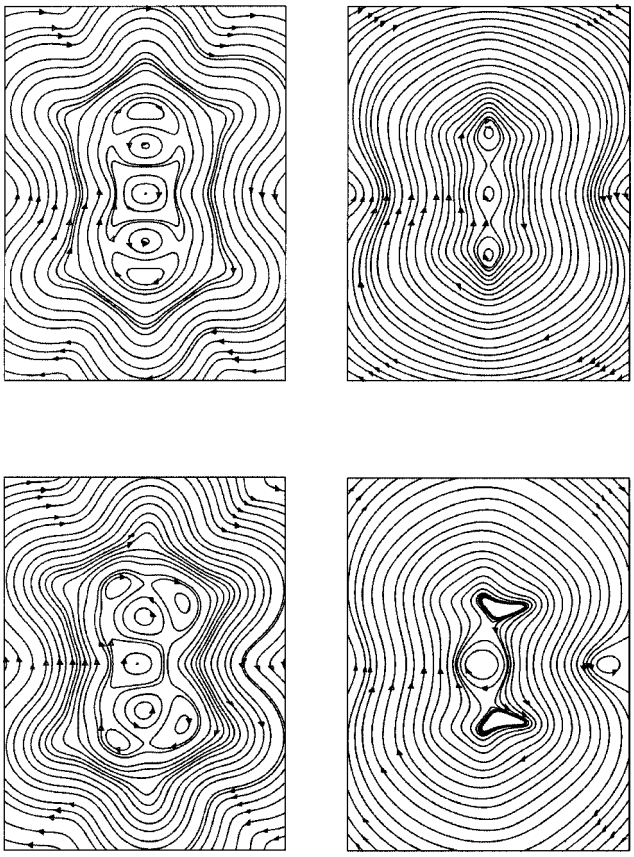

FIG. 4. Streamlines of the current density vector field in a plane parallel to that of the molecule, at the distance of 0.8 bohr, induced by a perpendicular magnetic field. The conventions are the same as in Fig. 1. The plots on the left (right) are for 1,6-dihydro-pyrrolo[2,3−*b*]pyrrole ([3,4−*c*] isomer). The trajectories for the total (π-electron contribution) are represented by left (right) of the figure.

III. VISUALIZATION OF DIATROPICITY BY CURRENT DENSITY MAPS

Maps of the electronic current density induced in 1,6-dihydro-pyrrolo[2,3−*b*]pyrrole, 1,4-dihydro-pyrrolo[3,2−*b*]pyrrole, and [3,4−*c*] isomer by an external magnetic field **B** perpendicular to the molecular plane (in the direction of the positive *z* axis), are shown in Figs. 1–4. They have been obtained via CTOCD-DZ coupled SCF calculations. The molecular domain investigated is that of maximum π density at $\approx$0.8 bohr above the plane of the nuclei.

A reduced set of streamlines that describes the essential features of electron circulation is shown for each molecule on top of Figs. 1–3. They provide quite simplified perspective pictures, which convey the information needed to assess the degree of diatropic character. In addition, they indicate that a significant leap-frog effect[30] takes place in the ring currents.

A more refined representation for the streamlines on the plane at 0.8 bohr is given in Fig. 4. A peculiar pattern characterizes the π current density in N-containing bis-heteropentalenes: most of the orbits encompass the entire molecule. They are fully delocalized over the molecular ring. Three internal diamagnetic vortices can be observed in the π current density of [2,3−*b*] and [3,4−*c*] systems in Fig. 4.

The collective clockwise motion of the π-electrons as a whole in the presence of a magnetic field at right angle to the plane of the molecule gives a *visual indicator* of diatropicity. Its qualitative feature is not less important and significant than other measures of aromaticity, if a connection between diatropicity and aromaticity really exists.

Also the plots of the modulus $|\mathbf{J}|=\rho|\mathbf{v}|$ yield relevant information and provide physical insight for understanding the unique magnetic properties of aromatics. Comparison with the corresponding plots for the charge density is illuminating. The maps clearly show the effect of the magnetic field on the π-cloud.

It is commonly held that the π-electrons of an aromatic molecule are *delocalized* all over the molecular domain. However, the plots of the π-charge at the right bottom of Figs. 1–3 indicate that $\rho(\mathbf{r})$ is a function characterized by maxima localized essentially in the proximity of C nuclei. On the contrary, the $|\mathbf{J}|$ modulus, represented above in the same figure, shows significant merging of adjacent domains of the π-charge distribution operated by the magnetic field.

As matter of fact, the sharp peaks in the proximity of the nuclei in the ρ field become much smoother in the plot of the corresponding $|\mathbf{J}|$. They are connected to one another by a ''pass,'' in the region of each bond, where the modulus of the π-current density is only slightly smaller than the nearby maxima on the $|\mathbf{J}|$ surface. Some speculations have been previously reported, suggesting that the local average velocity **v** over the bonds is higher than over the nuclei.[53]

The streamline field for the total current density, represented on the left top of Figs. 1–3, and on the left of Fig. 4, is characterized by a much more complicate topology. The maps show that the primary diamagnetic vortex circulating in the tail regions of the molecule branches out in the vicinity of the nuclear skeleton, giving rise to a set of internal vortices separated by saddle-type stagnation lines.

The pattern found for the [3,4−*c*] system is particularly interesting. Five vortices, having their center on the longitudinal axis of the molecule, and four saddles can be seen on the left top of Fig. 4. The topology is consistent with the Gomes theorem.[4] The internal diamagnetic vortex rotates about the center of mass, all over the C–C bond connecting two pyrrole rings. It is separated from the two diamagnetic vortices at the opposite ends of the longitudinal axis, in the proximity of the N nuclei, by a couple of adjacent paramagnetic vortices, flowing about the center of each pyrrole unit. These intermediate paramagnetic vortices are typical of every planar conjugated cyclic molecule.[5]

IV. CONCLUSIONS

The present study shows that CTOCD procedures for theoretical magnetic properties of medium size molecules like bis-heteropentalenes are effective tools, alternative to those adopting London orbitals. Comparison of calculated values demonstrates that basis sets of big size and high flexibility are required in any case to attain near HF accuracy.

A scale of relative diatropicity of bis-heteropentalenes formed by two fused pyrrole units can be built up assuming the out-of-plane component of the susceptibility tensor as an indicator. The degree of diatropicity of dihydro-pyrrolo–

Downloaded 16 Mar 2004 to 147.156.122.171. Redistribution subject to AIP license or copyright, see http://jcp.aip.org/jcp/copyright.jsp

pyrroles does not agree either with the sequence of SCF energies or TRE aromaticity measures: the $[3,4-c]$ isomer is the least aromatic, even if it shows the strongest diamagnetic ring currents.

A qualitative indicator, suitable for visualizing the diatropic character of bis-heteropentalenes, is given by plots for the trajectories of the electron flow induced by a magnetic field at right angles to the molecular plane and by corresponding maps for the modulus of the current density vector.

ACKNOWLEDGMENTS

The authors wish to thank Professor A. Rastelli for his help in geometry optimization. Financial support from the European research and training network ''Molecular Properties and Materials (MOLPROP),'' Contract No. HPRN-CT-2000-00013, from DGI (Dirección General de Investigación) of the Spanish MCyT (Ministerio de Ciencia y Tecnología) under Project No. BQU2001-2935-C02-01, and from the Italian MURST (Ministero dell'Università e della Ricerca Scientifica e Tecnologica), via 60% funds, is gratefully acknowledged.

[1] P. von Ragué Schleyer, P. K. Freeman, H. Jiao, and B. Goldfuss, Angew. Chem., Int. Ed. Engl. **34**, 337 (1995).
[2] A. R. Katrizky, P. Barczynski, G. Musumarra, D. Pisano, and M. Szafran, J. Am. Chem. Soc. **111**, 7 (1989).
[3] P. von Ragué Schleyer, Chem. Rev. **101**, 1115 (2001).
[4] J. A. N. F. Gomes and R. B. Mallion, Chem. Rev. **101**, 1349 (2001).
[5] P. Lazzeretti, ''Ring currents,'' *Progress in Nuclear Magnetic Resonance Spectroscopy* (Elsevier, New York, 2000), Vol. 36, pp. 1–88.
[6] K. Jug and A. M. Köster, J. Phys. Org. Chem. **4**, 163 (1991).
[7] M. Cyrañski, T. M. Krygowski, A. R. Katrizky, and P. von Ragué Schleyer, J. Org. Chem. **67**, 1333 (2002).
[8] M. J. S. Dewar and N. Trinajstić, J. Am. Chem. Soc. **92**, 1453 (1970).
[9] R. Gleiter, M. Kobayashi, J. Spanget-Larsen, S. Gronowitz, A. Konar, and M. Farnier, J. Org. Chem. **42**, 2230 (1977).
[10] B. M. Gimarc, J. Am. Chem. Soc. **105**, 1979 (1983).
[11] C. W. Bird, Tetrahedron **43**, 4725 (1987).
[12] T. Kobayashi, K. Ozaki, and S. Yoneda, J. Am. Chem. Soc. **110**, 1793 (1988).
[13] Z. Zhou and R. G. Parr, J. Am. Chem. Soc. **111**, 7371 (1989).
[14] I. Novak, J. Mol. Struct.: THEOCHEM **398–399**, 315 (1997).
[15] C. W. Bird, Tetrahedron **41**, 1409 (1985).
[16] C. W. Bird, Tetrahedron **48**, 335 (1992).
[17] G. Subramanian, P. von Ragué Schleyer, and H. Jiao, Angew. Chem., Int. Ed. Engl. **35**, 2638 (1996).
[18] I. Gutman, M. Milun, and N. Trinajstić, J. Am. Chem. Soc. **99**, 1692 (1977).
[19] P. W. Fowler and E. Steiner, J. Phys. Chem. A **101**, 1409 (1997).
[20] E. Steiner and P. W. Fowler, J. Phys. Chem. A **105**, 9553 (2001).
[21] P. W. Fowler and E. Steiner, Chem. Phys. Lett. **364**, 259 (2002).
[22] E. Steiner and P. W. Fowler, J. Chem. Soc., Chem. Commun. 2220 (2001).
[23] L. Pauling, J. Chem. Phys. **4**, 673 (1936).
[24] K. Lonsdale, Proc. R. Soc. London, Ser. A **159**, 149 (1937).
[25] F. London, J. Phys. Radium **8**, 397 (1937), 7ème Série.
[26] F. London, J. Chem. Phys. **5**, 837 (1937).
[27] R. H. Mitchell, Chem. Rev. **101**, 1301 (2001).
[28] E. Steiner, P. W. Fowler, and L. W. Jenneskens, Angew. Chem., Int. Ed. Engl. **40**, 362 (2001).
[29] R. W. A. Havenith, L. W. Jenneskens, and P. W. Fowler, Chem. Phys. Lett. **367**, 468 (2003).
[30] A. Ligabue, A. Soncini, and P. Lazzeretti, J. Am. Chem. Soc. **124**, 2008 (2002).
[31] F. B. van Duijneveldt, ''Gaussian basis sets for the atoms H–Ne for use in molecular calculations,'' Research Report RJ 945, IBM, 1971.
[32] R. Zanasi and P. Lazzeretti, J. Chem. Phys. **85**, 5924 (1986).
[33] M. J. Frisch, G. W. Trucks, H. B. Schlegel *et al.*, GAUSSIAN 94, Revision B.3, Gaussian, Inc., Pittsburgh, PA, 1995.
[34] J. Andzelm and E. Wimmer, J. Chem. Phys. **96**, 1280 (1992).
[35] H. tom Dieck, U. Vefürth, K. Dilbitz, and G. Fendesak, Chem. Ber. **122**, 129 (1989).
[36] P. C. Hariharan and J. A. Pople, Theor. Chim. Acta **28**, 213 (1973).
[37] T. H. Dunning, Jr., J. Chem. Phys. **90**, 1007 (1989).
[38] P. Lazzeretti, M. Malagoli, and R. Zanasi, Technical report on project ''sistemi informatici e calcolo parallelo,'' Research Report 1/67, CNR, 1991.
[39] T. A. Keith and R. F. W. Bader, Chem. Phys. Lett. **210**, 223 (1993).
[40] T. A. Keith and R. F. W. Bader, J. Chem. Phys. **99**, 3669 (1993).
[41] T. A. Keith and R. F. W. Bader, Can. J. Chem. **74**, 185 (1996).
[42] R. F. W. Bader and T. A. Keith, Int. J. Quantum Chem. **60**, 373 (1996).
[43] P. Lazzeretti, M. Malagoli, and R. Zanasi, J. Chem. Phys. **102**, 9619 (1995).
[44] P. Lazzeretti and R. Zanasi, Int. J. Quantum Chem. **60**, 249 (1996).
[45] R. Zanasi, J. Chem. Phys. **105**, 1460 (1996).
[46] A. E. Hansen and T. D. Bouman, J. Chem. Phys. **82**, 5035 (1985), this is the first reference in which the reinterpretation of the GIAO acronym for gauge-including-atomic-orbitals has been proposed, see footnote 6, p. 5047.
[47] T. Helgaker, H. J. A. Jensen, P. Jørgensen *et al.*, Dalton, An electronic structure program, Release 1.2, Dalton, 2001.
[48] P. Lazzeretti, M. Malagoli, and R. Zanasi, Chem. Phys. Lett. **220**, 299 (1994).
[49] S. Coriani, P. Lazzeretti, M. Malagoli, and R. Zanasi, Theor. Chim. Acta **89**, 181 (1994).
[50] R. Zanasi, P. Lazzeretti, M. Malagoli, and F. Piccinini, J. Chem. Phys. **102**, 7150 (1995).
[51] R. Zanasi, P. Lazzeretti, and P. W. Fowler, Chem. Phys. Lett. **278**, 251 (1997).
[52] J. Hoarau, N. Lumbroso, and A. Pacault, C. R. Acad. Sci. Paris **242**, 1702 (1956).
[53] A. Ligabue and P. Lazzeretti, J. Chem. Phys. **116**, 964 (2002).
[54] R. S. Jartín, A. Ligabue, A. Soncini, and P. Lazzeretti, J. Phys. Chem. A **106**, 11806 (2002).
[55] A. Ligabue and P. Lazzeretti, J. Chem. Phys. **116**, 964 (2002); EPAPS material available at http://www.aip.org/pubservs/epaps.html
[56] J.-I. Aihara, Pure Appl. Chem. **54**, 1115 (1983).
[57] J.-I. Aihara, J. Am. Chem. Soc. **101**, 5913 (1979).
[58] J. Aihara, J. Am. Chem. Soc. **103**, 5704 (1981).
[59] J.-I. Aihara and T. Horikawa, Chem. Phys. Lett. **95**, 561 (1983).
[60] J.-I. Aihara and T. Horikawa, Bull. Chem. Soc. Jpn. **56**, 1853 (1983).
[61] J.-I. Aihara, J. Am. Chem. Soc. **107**, 298 (1985).
[62] H. Hosoya, Theor. Chim. Acta **25**, 215 (1972).

Downloaded 16 Mar 2004 to 147.156.122.171. Redistribution subject to AIP license or copyright, see http://jcp.aip.org/jcp/copyright.jsp